THE AMERICAN SOCIETY OF MECHANICAL ENGINEERS
345 E. 47 St., New York, N.Y. 10017

86-WA/Sol-1

#6783

Interzonal Natural Convection for Various Aperture Configurations

BAL M. MAHAJAN and DALLAS D. HILL
Solar Equipment Group
National Bureau of Standards
Gaithersburg, MD 20899

ABSTRACT

Experiments were conducted to study the interzonal natural convection for different aperture configurations for a two-zone set-up. The following four aperture configurations were studied: (1) A center door; (2) a side door; (3) a window; and (4) a split window, i.e, two small windows situated symmetrically about the horizontal bisector of the common wall. One of the two zones was heated with baseboard electric heaters placed adjacent to the floor along the wall opposite to the common wall. Experiments were conducted with various heat inputs to the warmer of the two zones. The data indicate that the flow coefficients used in simple one-dimensional model for interzonal airflow varies with the aperture configuration and the level of heat input to the warmer zone. Variations in the flow coefficients are apparently due to the different flow fields and temperature distributions for each aperture configuration.

NOMENCLATURE

A_a = Aperture cross section area (m^2)
A_w = Cross section area of the wall containing the aperture (m^2)
C = Discharge coefficient or aperture mass flow coefficient (non-dimensional)
C_p = Specific heat or air (j/kg °K)
C_t = Temperature correction coefficient (non-dimensional)
g = Acceleration due to gravity (m/s^2)
H = Height of the aperture, see figure 3. (m)
L = Vertical distance from center of wall to the bottom of the split window, defined in figure 3 (m)
M = Mass flow rate (kg/s)
M_r = Reference value of mass flow rate (kg/s)
Q = Heat Transfer rate (W)
Q_r = Reference value of heat transfer rate (W)
T_1 = Average value of temperature in zone 1 (°K)
T_2 = Average value of temperature in zone 2 (°K)
$\bar{T}$ = $(T_1 + T_2)/2$ (°K)
$\bar{T}_r$ = Reference value of $\bar{T}$ (°K)
ΔT = $(T_1 - T_2)$, zone-to-zone temperature difference (°K)
ΔT_r = 1°K, reference value of zone-to-zone temperature difference
U = Magnitude of air velocity in the aperture m/s
U_m = Magnitude of the maximum possible air velocity (m/s)
W = Width of the aperture (m)
Y = Vertical distance from the mid-height of the aperture (m) (Figure 3)
Y_m = H/2 (m)
ρ = Density of air at a temperature equal to $\bar{T}$ (kg/m^3)

Subscript

1 = zone 1, warmer of the two zones
2 = zone 2, cooler of the two zones
m = maximum value
r = reference value

Superscript

* = non-dimensionalized quantity

INTRODUCTION

Interzonal natural convection plays a major role in the distribution of heat in passive solar buildings. Thermal performance and comfort in passive solar buildings can be improved if apertures are configured/designed properly for effective interzonal convective heat transfer. Hence, methods for predicting the interzonal natural convective heat transfer through different aperture configurations are needed.

The existing one-dimensional models [1-7] for predicting the interzonal natural convection cannot properly account for the three-dimensional aspects of the flow and the boundary constraints at the aperture boundaries. But the use of flow coefficients (a

Presented at the Winter Annual Meeting
Anaheim, California — December 7-12, 1986

discharge coefficient for velocity and mass transfer, and a temperature coefficient for heat transfer) in one-dimensional models makes it possible to bring the predicted and measured values within reasonable agreement. Hence, the use of empirically determined discharge coefficients for different experimental configurations may enable an estimate of the interzonal natural convective heat transfer by using the existing simple one-dimensional model.

In recent experimental studies conducted at the National Bureau of Standards (NBS) [8-10], it was found that for a doorway the value of discharge coefficient, C, to be used in the simple one-dimensional model varied between 0.45 and 0.54. These values are 11 to 26% lower than the commonly recommended value of 0.61 [1-3] and 20 to 34% lower than a value of 0.68 given in reference 7. This difference in the discharge coefficient values appears to be due to the difference in the experimental set-up and aperture configurations. Therefore, it was decided to experimentally determine the values of flow coefficients for other aperture configurations under different test conditions. Experiments were conducted for four aperture configurations with four levels of heat input to the warmer of the two zones. This paper will briefly describe the aperture configuration and measurement procedure, and present representative results.

SIMPLE MODEL

The one-dimensional model presented below follows the theory developed in references 1 to 7. Assuming that the interzonal airflow through the aperture is steady and zone-to-zone temperature difference is independent of vertical distance, Y, the magnitude, U, of the local air velocity along a streamline in the aperture may be expressed as:

$$U = C\ (2gY\Delta T/\bar{T})^{0.5} \tag{1}$$

Equation (1) may be rewritten in non-dimensional form as:

$$U^* = U/U_m = C(Y^*)^{0.5} \tag{2}$$

$$U_m = (2gY_m\Delta T/\bar{T})^{0.5} \tag{3}$$

Where U_m is the maximum possible velocity for a given value of Y_m, ΔT and $\bar{T}$. The coefficient C, is an aperture mass flow coefficient (or a discharge coefficient) which accounts for the viscous losses at the area contraction. The interzonal mass flow rate, M, is obtained by integration of the local velocity between y = o and $y = y_m$, and may be expressed as:

$$M = C(2/3)(\rho W Y_m^{1.5})(2g\Delta T/\bar{T})^{0.5} \tag{4}$$

Equation (4) gives mass flow rate for both the outflow (i.e., the flow of warm air to the cooler zone) and the inflow (i.e., the flow of cool air to the warmer zone). Equation (4) may be written in non-dimensional form as:

$$M^* = M/M_r = C\ (\Delta T^*/T^*)^{0.5} \tag{5}$$

$$M_r = (2/3)(\rho W Y_m^{1.5})(2g\Delta T_r/\bar{T}_r)^{0.5} \tag{6}$$

Where, M_r is the reference value of mass flow rate for a given aperture configuration (i.e., W and Y_m) computed for a reference value of zone-to-zone temperature difference, ΔT_r, and reference average temperature, $\bar{T}_r$. For the purpose of this study, we assume that ΔT_r = 1°K, and $\bar{T}_r$ = 295°K (a value very close to the actual value of $\bar{T}$ for the experiments described in this paper).

The associated heat transfer rate through the aperture may be expressed as:

$$Q = C_t\ C_p M \Delta T \tag{7}$$

Equation (7) may be written in non-dimensional form as:

$$Q^* = Q/Q_r = C\ C_t\ (\Delta T^{*3}/T^*)^{0.5} \tag{8}$$

$$Q_r = C_p M_r \Delta T_r \tag{9}$$

Where, Q_r is the reference value of heat transfer rate for a given aperture. The quantity C_t is a temperature correction coefficient, it accounts for the difference in the value of average air temperature based on the zone temperatures and the average temperature of air in the aperture. A quantity similar to the quantity C_t has been used by other researchers [3,6,9].

Earlier results [3,5,6 to 10) suggest that the simple one-dimensional model discussed above can adequately predict the interzonal natural convection for any aperture configuration if the proper values of coefficients C and C_t are used in the respective equations.

DESCRIPTION OF THE EXPERIMENTS

Full scale natural convection experiments were conducted at the NBS Passive Solar Test Facility. A floor plane of the building is shown in figure 1.

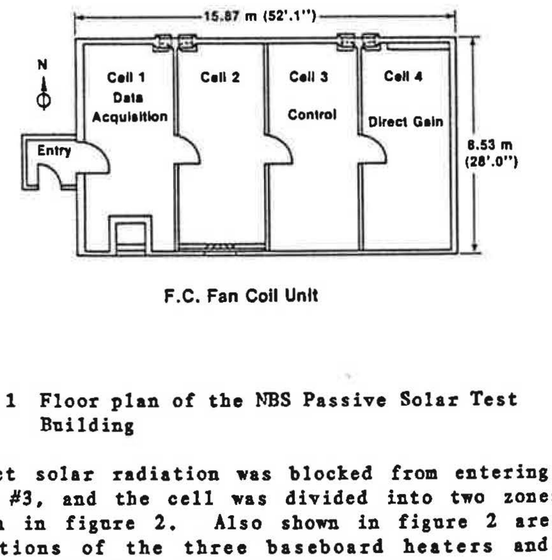

FIG. 1 Floor plan of the NBS Passive Solar Test Building

Direct solar radiation was blocked from entering the cell #3, and the cell was divided into two zones as shown in figure 2. Also shown in figure 2 are the locations of the three baseboard heaters and the strings of nine thermocouples used to monitor the temperatures. The wall separating the two zone, i.e, the common wall, was constructed with sheets of 5.1 cm (2 in.) thick extruded polystyrene which easily provided for the construction of different aperture configurations. The four aperture configurations used in these experiments are shown schematically in figures 3. These include: (1) a center door; (2) a side door; (3) a window; and (4) a split window.

The velocity and temperature distributions of the airflow through the aperture were measured with six hot wire anemometers and six thermocouples located along

t = ΔT ≠ f(t)
Q = Ct Cp M Δq
↑ wrong Δt.

TABLE 1 Summary of test conditions for different experiments

Heat Input into Zone #1 During the Test (watts)	Location of Heater That is On	Aperture Configurations Tested 1 Center Door A_a/A_w = .16	2 Side Door A_a/A_w = .16	3 Window A_a/A_w = .08	4 Split Window A_a/A_w = .07
0	O	■	■	■	■
500	H_2	■	■	■	■
1,000	H_1, H_3	■	■	■	■
1,500	H_1, H_2, H_3	■	■	■	■

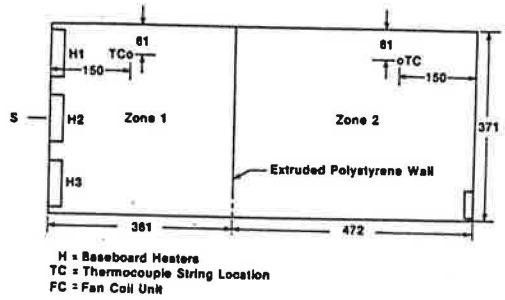

FIG 2 Schematic floor plan of the experimental area

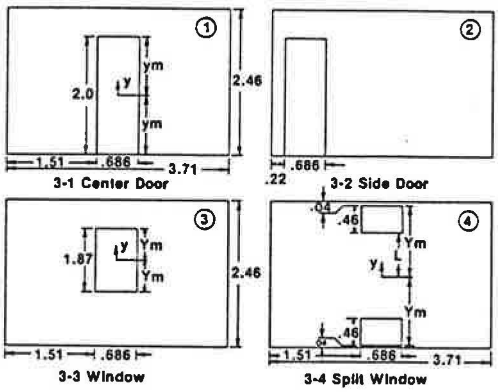

FIG 3 Schematic of the common wall showing the four aperture configurations tested

the vertical centerline of the aperture. Temperatures were measured with type -T thermocouples. The maximum uncertainty is estimated to be 0.5°C in the temperature measurements and 0.025 m/s in the air speed measurements.

Before starting an experiment, the aperture was blocked with a removable extruded polystyrene panel. Zone #1 was heated by heat supplied by the electric baseboard heaters, while zone #2 was cooled using a fan coil cooling unit. When the average zone-to-zone temperature difference was greater than 12°C, the auxiliary cooling in zone #2 was turned off and the panel blocking the aperture was removed to start the experiment. The status of the heat input into zone #1 (i.e., warmer of the two zones) for different experiments is summarized in Table 1. Data were then collected every two minutes for a period of three hours.

RESULTS AND DISCUSSION

As summarized in Table 1, interzonal natural convection experiments were performed for four aperture configurations. For each configuration tests were conducted with four levels of heat input to the warmer of the two zones (i.e., zone #1) during the experiments. Representative data from the tests are presented in figures 4 through 13.

Air Temperatures and Velocities

The average value of air temperatures T_1, and T_2 were computed from the readings of the nine air temperature sensing thermocouples in respective zone. These values of T_1 and T_2 were used to compute the values of zone-to-zone temperature difference, ΔT, and the overall average air temperature, $\bar{T}$. Figure 4 shows the zone-to-zone temperature difference ΔT for various elapsed times for four levels of heat input for aperture configuration 3, i.e, the window. These data indicate that the value of ΔT drops rapidly during the first half to one hour, and the rate of drop in the value of ΔT decreased with elapsed time as the air in the two zones mixes. Zone-to-zone temperature difference data for the experiments conducted for other aperture was similar to the data shown in figure 4.

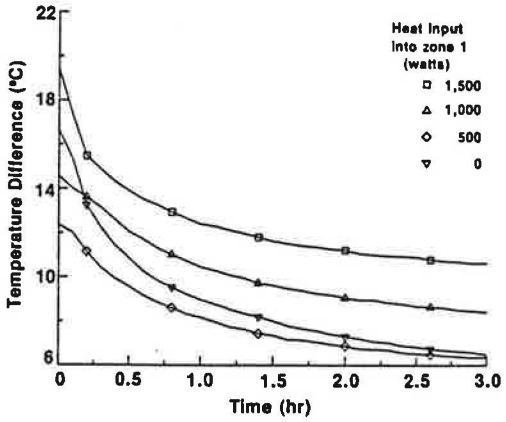

FIG 4 Zone-to-zone temperature difference for various elapsed times for all four test conditions for the window

In figure 5, data taken 30 minutes after the start of the test are shown for the window (i.e., aperture configuration 3) for no heat input into zone #1 during the test. The instantaneous data are displayed on a north-south cross section of the experimental enclosure with the temperature scale located at the bottom of the figure and the enclosure height on the left side. In the center of the figure the aperture is shown with velocity scale located at the top of the aperture. The aperture velocity distribution is represented by the solid line and the temperature distribution by line marked with circles. The zone temperature distributions, monitored with a string of nine thermocouples in each zone, are displayed in the respective zone. These data indicate the temperature distribution in both zones is non-linear. The data for other elapsed times for this aperture and for other experiments were similar in trend to the data of figure 5; although the temperature distribution in each zone and the aperture differed for different apertures because of the different natural air circulation loops.

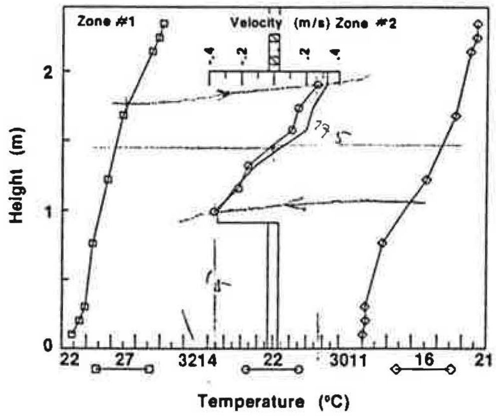

FIG 5 Instantaneous temperature and velocity distribution for an elapsed time of 30 minutes, for the window with no heat input into zone #1

The velocity of the outflow (i.e., the flow from warmer zone to the cooler zone) is taken as positive, while the velocity of the inflow is taken as a negative. Figure 6 shows aperture velocity distribution for different experiments for the window. These data were taken 30 minutes after the start of each experiment. These data indicate the velocity is fairly symmetrical with respect to neutral plane (i.e, the plane of zero velocity). However, the neutral plane is slightly below the geometric center of the aperture and the outflow velocities are slightly lower than the inflow velocities. The difference in the magnitude of velocities for different tests is due to the difference in the corresponding values of ΔT (figure 4).

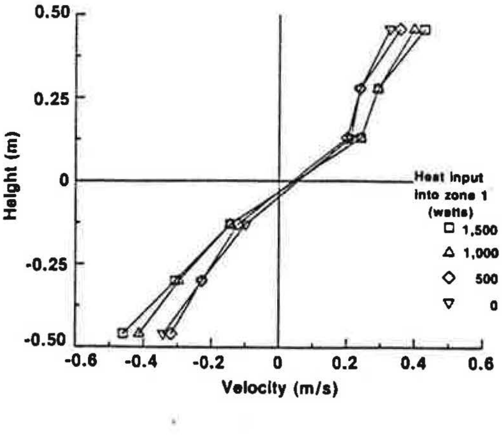

FIG 6 Velocity distribution for an elapsed time of 30 minutes, for the window for all four test conditions

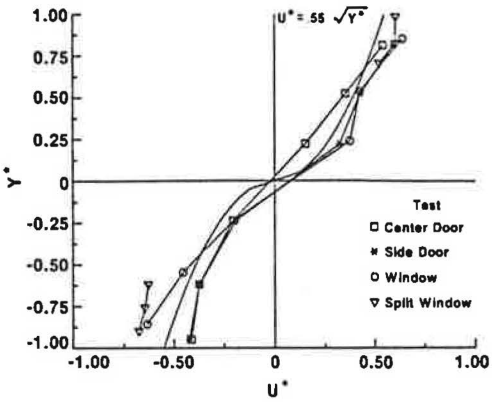

FIG 7 Non-dimensional velocity for an elapsed time of 30 minutes, for the four apertures, for tests with 1500 watts of heat input into zone 1

Figure 7 shows the non-dimensionalized velocity data for an elapsed time of 30 minutes for all four apertures. These data are from the experiments with 1500 watts of heat input into zone #1 during the tests. Equation (2) is also plotted on this figure for the purpose of comparison. It is seen that the measured velocity distributions, due to the different flow constraints at the aperture boundaries, are different for different apertures. The boundary constraints cannot be properly accounted for in the simple model. The measured data for the window configurations are fairly symmetrical with respect to the natural plane as predicted by equation (2). The data for both of the door configurations show that due to curving of the streamlines outflow velocity near the top edge of the aperture is higher than predicted by equation (2); while due to the no slip constraint at the floor the inflow velocity near the bottom edge of the aperture is lower than predicted by equation (2). These doorway velocity profiles are quite similar to the doorway velocity profiles measured during FY 1985 experiments for a different test configuration [8, 9 nd 10].

Mass and Heat FLow Rates

The experimental mass flow rates were computed from the velocity and temperature data taken at various heights in the aperture. The product of the local velocity, density and area was summed using trapezoidal summation techniques. The difference in the values of mass flow rates for the inflow and the outflow thus computed was 10% or less for all data. The experimental mass flow rate was non-dimensionalized by dividing it by the reference value of mass flow rate for the respective aperture. It should be noted that for the split window the quantity ($Y_m^{1.5}$) in equation (4) and (6) needs to be replaced with the quantity ($Y_m^{1.5} - L^{1.5}$). The measured values of zone-to-zone temperature difference, ΔT, and average temperature, $\bar{T}$, were also non-dimensionalized by dividing these quantities with the respective reference quantities. Experimental heat flow rate was computed from the aperture velocity and temperature data, and non-dimensionalized.

Typical mass and heat flow rate data are shown in figures 8 to 13. The non-dimensionalized mass flow rate are plotted as functions of the quantity $(\Delta T^{*}/T^{*})^{0.5}$, while non-dimensional heat flow rate data are displayed as functions of the quantity $(\Delta T^{*3}/T^{*})^{0.5}$. A linear least square curve fitting technique was used to determine the values of discharge coefficient, C, for equation (5) and temperature correction coefficient, C_t, for equation (8). The values of flow coefficients, C and C_t, for all 16 experiments are given in Table 2.

Figures 8 and 11 respectively show mass and heat flow rate data for window for all four test conditions. Figures 9 and 12 respectively show mass and heat flow rate data for all four apertures for tests with no heat input into zone #1 during the test. Figures 10 and 13 respectively show mass and heat flow rate data for all four apertures for tests with 1500 watts of heat input into zone #1 during the tests. It is seen that the values of discharge coefficient, C, for the two door configurations are about the same; while the values of C for the two window configurations are the same except for the tests with all three heaters on in zone #1. The value of discharge coefficient, C, found for a doorway, from our FY 1985 data [8, 9 and 10], for a different test set-up varied between 0.47 to 0.54. The doorway area to wall area ratio for these experiments (≈0.15) is different from that of our earlier experiments (≈.07). The available data are too few to determine a definitive relationship, if any, between C and aperture to wall area ratio although it appears that C increases with a decrease in the aperture to wall area ratio. The value of the discharge coefficient does increase with the increase in the heat input to the warmer zone during the tests because the addition of heat to zone #1 during the test affects the zone and aperture temperature distribution.

The values of the temperature correction coefficient, C_t, for the window are much less than the values of C_t for other apertures. For the window, the values of C_t are all nearly equal to unity except for the test with no heat supply to zone #1 during the test. Because of the central location of the window, it seems reasonable that the zone temperature distribution has little or no effect on C_t. The values of C_t for all other apertures are greater than unity; and the value of C_t is larger for the tests with heat on in zone #1 than it is for the tests with no heat supply.

The value of C_t given in Table 2 shows that the variation in the value of C_t with increase in the amount of heat input to zone #1 does not display a definitive trend. It appears that the location of heat input, i.e., location of the heaters with respect to the aperture, also affect the value of C_t; probably because the different locations of heat input modify the temperature in Zone #1 and the aperture differently. These three dimensional aspects of the temperature field are difficult to map, and cannot be accounted for in a one-dimensional model. The available data are too few to establish any definitive relationship between the flow coefficients (C and C_t) and the amount of heat input to the warmer zone during the test.

It is seen in figures 8 through 13 that the interzonal mass and heat flow rates are adequately represented respectively by equations (5) and (8). These results suggest that the simple one-dimensional model can adequately predict the interzonal natural convection for any configuration if the proper values of the coefficients C and C_t are used in the respective equation.

TABLE 2 Values of C and C_t determined from data for different tests

Heat Input into Zone #1 (watts)	Values of C for the Aperture Configuration: 1 Center Door	2 Side Door	3 Window	4 Split Window	Values of C_t for the Aperture Configuration: 1 Center Door	2 Side Door	3 Window	4 Split Window
0	.33	.36	.49	.47	1.2	1.44	0.83	1.28
500	.34	.38	.53	.53	1.72	1.76	1.09	1.89
1,000	.34	.38	.58	.58	2.01	1.66	0.97	1.60
1,500	.42	.48	.58	.59	1.76	1.87	0.83	1.34

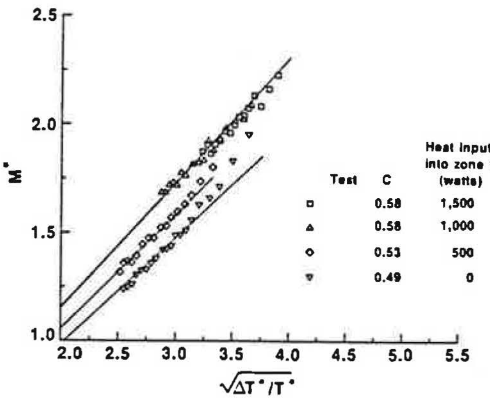

FIG 8 Non-dimensional interzonal mass flow rate as function of non-dimensional zone-to-zone temperature different, for the window for the four test condtions

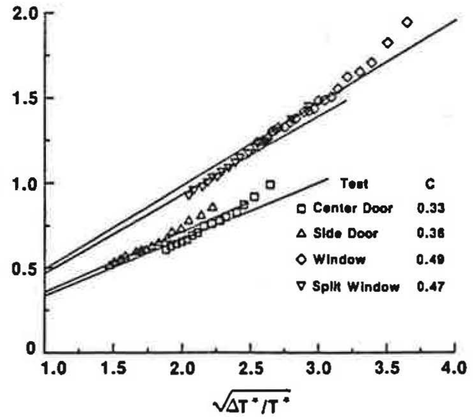

FIG 9 Non-dimensional interzonal mass flow rate as a function of non-dimensional zone-to-zone temperature difference for the four apertures for tests with no heat input into zone #1

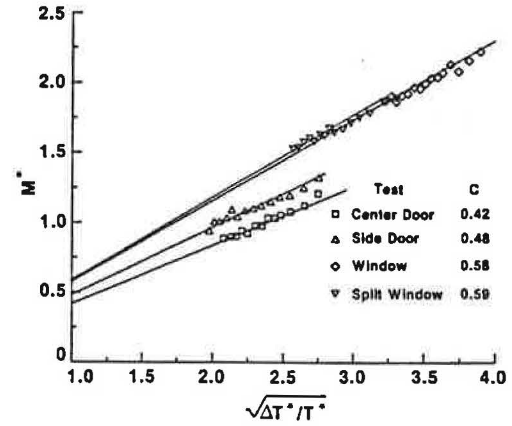

FIG 10 Non-dimensional interzonal mass flow rate as a function of non-dimensional zone-to-zone temperature difference for the four apertures, for the test with 1500 watts of heat input into zone #1

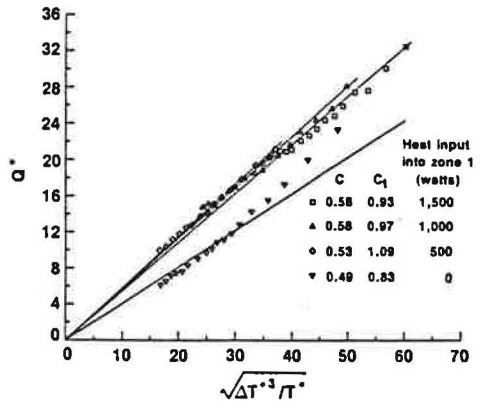

FIG 11 Non-dimensional interzonal heat flow rate as a function of non-dimensional zone-to-zone temperature difference for the window, for the four test conditions

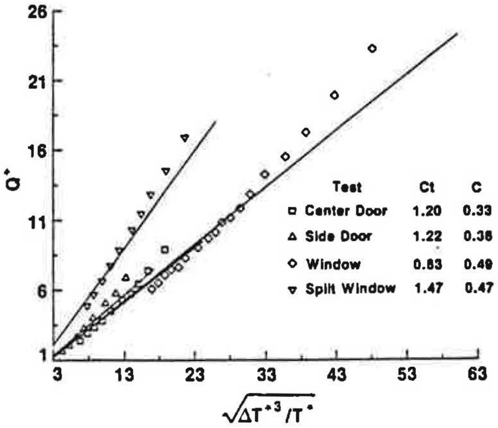

FIG 12 Non-dimensional interzonal heat flow rate as a function of non-dimensional zone-to-zone temperature difference for the four apertures, for no heat input into zone #1

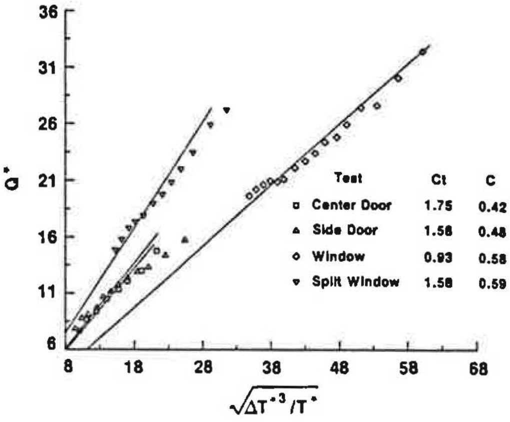

FIG 13 Non-dimensional interzonal heat flow rate as a function of non-dimensional zone-to-zone temperature difference for the four apertures, for 1500 watts of heat input into zone #1

CONCLUSIONS

Based on the data presented, the following statements may be made. The interzonal natural convection can be adequately predicted by the one-dimensional model for any aperture configuration if appropriate values of the flow coefficients, C and C_t are known. The discharge coefficient appears to increase with a decrease in the aperture to wall area ratio, and an increase in the heat input to the warmer zone during the test; but the data are too few to develop any relationship. The temperature correction coefficients appear to be dependent on the aperture configuration as well as on the location and the amount of heat supply to the warmer zone during the test; data are too few to develop any definitive relationships. Further experimental research is needed to collect more data for developing relationships between the flow coefficients, C and C_t, and aperture configuration and test conditions.

ACKNOWLEDGMENT

This work is sponsored by the Passive and Hybrid Solar Energy Division, Office of Solar Heat Technologies, U. S. Department of Energy, Washington, D.C. 20585, as part of the experimental systems research program. The authors wish to express their sincere gratitude to Mr. Donn E. Ebberts for his valuable contributions in instrument installation, and Mrs. Flora J. Parsons for her timely preparation of the manuscript.

REFERENCES

1. Brown, W. A. and Solvason, K. R., "Natural Convection Through Rectangular Opening in Partitions - 1 Vertical Partitions," Int. J. Heat and Mass Transfer, 1962, 5, 859.

2. Walton, A. N., "A Computer Algorithm for Estimating Infiltration and Inter-Room Air Flow," NBSIR 83-2635, Nov. 1982.

3. Balcomb, J. D., Jones, A. F. and Yamaguchi, K., "Natural Air Motion and Stratification in Passive Buildings," Proc. of Passive and Hybrid Solar Energy Update, Washington, D.C., Sept. 5-7, 1984.

4. Weber, D. D., "Similitude Modeling of Natural Convection Heat Transfer Through an Aperture in Passive Solar Heated Building," LASL Report LA-8385-T, June 1980.

5. Hill, D.; Kirkpatrick, A. and Burns, P., "Interzonal Natural Convection Heat Transfer in a Passive Solar Building," ASME/AICHE National Heat Transfer Conference, Denver, CO, August 1985.

6. Jones, G. F.; Balcomb, J. D. and Otis, D. R., "A Model for Thermally Driven Heat and Air Transport in Passive Solar Buildings," ASME Winter Annual Meeting, Miami Beach, Florida, November 1985.

7. Steckler, K. D.; Baum, H. R. and Quintiere, J. A., "Fire Induced Flows Through Room Openings -Flow Coefficients," NBSIR 83-2801, March 1984.

√ 8. Mahajan, B. M., "Inter-room Air Flow by Natural Convection via a Doorway Opening," Proc. of the 1986 ASME Solar Energy Division Conference, Anaheim, California, April 14-17, 1986.

9. Hill, D. D.; and Mahajan, B. M., "Convection Between Zones with Non-linear Temperature Distribution,", Proc. of the Air Movement and Distribution Conference, Purdue University, Lafayette, Ind., May 27-29, 1986.

10. Mahajan, B. M,; "Measurement of Air Velocity Components of Natural Convective Interzonal Airflow,", Proc. of the Air Movement and Distribution Conference, Purdue University, Lafayette, Ind., May 27-29, 1986.